Available online at www.sciencedirect.com
ScienceDirect
Journal of Organometallic Chemistry 692 (2007) 4506–4518
Journal of Organometallic Chemistry
www.elsevier.com/locate/jorganchem

Synthesis and characterization of iron and cobalt dichloride bearing 2-quinoxalinyl-6-iminopyridines and their catalytic behavior toward ethylene reactivity

Wen-Hua Sun [a,*], Peng Hao [a], Gang Li [a,b], Shu Zhang [a], Wenqing Wang [a], Jianjun Yi [c], Maliha Asma [a], Ning Tang [b,*]

[a] Key Laboratory of Engineering Plastics and Beijing National Laboratory for Molecular Sciences, Institute of Chemistry, Chinese Academy of Sciences, Beijing 100080, China
[b] State Key Laboratory of Applied Organic Chemistry, Lanzhou University, Lanzhou 730000, China
[c] Petrochemical Research Institute, PetroChina Company Limited, No. 20 Xueyuan Road, Beijing 100083, China

Received 14 February 2007; received in revised form 16 April 2007; accepted 20 April 2007
Available online 25 April 2007

Dedicated to Prof. Dr. Gerhard Erker on the occasion of his 60th birthday.

Abstract

The 1-(6-(quinoxalin-2-yl)pyridin-2-yl)ethanone was synthesized in order to prepare a series of *N*-(1-(6-(quinoxalin-2-yl)pyridine-2-yl)ethylidene)benzenamines (**L1**–**L7**), which provided new alternative N^N^N tridentate ligands coordinating with iron(II) and cobalt(II) dichloride to form complexes of general formula $LFeCl_2$ (**1**–**7**) and $LCoCl_2$ (**8**–**14**). All organic compounds were fully characterized by NMR, IR spectroscopic and elemental analysis along with and magnetic susceptibilities and metal complexes were examined by IR spectroscopic and elemental analysis, while their molecular structures (**L1**, **L4**, **1**, **4**, **10**, **13**) were confirmed by single crystal X-ray diffraction analysis. Upon activation with methylaluminoxane (MAO), all iron complexes gave good catalytic activities for ethylene reactivity (oligomerization and polymerization), while their cobalt analogues showed moderate activities toward ethylene oligomerization with modified methylaluminoxane (MMAO). Various reaction parameters were investigated for better catalytic activities, the higher activities were observed at elevated ethylene pressure. The iron and cobalt complexes with *para*-methyl substituents of aryl group linked on imino group showed highest activity.

Keywords: 2-Quinoxalinyl-6-iminopyridines; Iron and cobalt complex; Ethylene oligomerization; Ethylene polymerization

1. Introduction

The importance of α-olefins as substances with various applications has generally been recognized, and they are mainly produced by three full range processes of ethylene oligomerization by BP, Chevron Phillips and Shell companies [1] in addition to on-purpose range process of Phillips [2] and Sasol process [3] for ethylene trimerization or tetramerization. Driven by academic and industrial considerations, new catalysts and catalytic systems are pursued for high catalytic activity and high linear α-olefins selectivity. Inspired by the SHOP process using nickel complex bearing P^O ligands as catalyst [1b,1c,4], nickel complexes as catalysts have drawn much attentions and their progress has been well documented in recent several review articles [5]. Breakthroughs in organometallic chemistry and new metal complexes as catalysts for ethylene catalytic reactions were recorded with the pioneering works by Gibson group and Brookhart group employing bis(imino)pyridyl iron and cobalt complexes as highly active catalysts for

* Corresponding authors. Tel.: +86 10 62557955; fax: +86 10 62618239 (W.-H. Sun).
E-mail address: whsun@iccas.ac.cn (W.-H. Sun).

0022-328X/$ - see front matter © 2007 Elsevier B.V. All rights reserved.
doi:10.1016/j.jorganchem.2007.04.027

ethylene polymerization [6] and oligomerization [7]. Extensive research on bis(imino)pyridyl iron complexes has been focused upon the understanding of the active species or intermediates [8], controlling the products of polymers and oligomers and improving the catalytic activities through varying the steric and electronic characteristics of complexes [5a,5c,5e,9]. Especially, iron and cobalt catalysts for ethylene reactivities showed not only highly catalytic activities but also the unique properties of resultant polyethylene or oligomers with highly linear and vinyl-type features, which rooted to the absence of "chain walking" during ethylene insertion and is characteristically different from nickel catalytic system. Currently, there is only 1-butene annually separated with 87 kilotons in Chinese refinery factories while all other α-olefins are imported. With the advantage of high selectivity of linear α-olefins by catalytic system of bis(imino)pyridyl iron complexes, a full range process of ethylene oligomerization has been scaling-up with the joint-investment by PetroChina and DuPont in order to have first commercial process of ethylene oligomerization catalyzed by iron complexes in China. Searching alternative models of iron and cobalt catalysts, however, had not awarded reasonable credits to scientists due to the lower catalytic activities [7f,10]. On the base of 1,10-phenanthroline, fortunately, the frameworks showed promising results of their metal complexes as catalysts for ethylene reactivities. Though the iron and cobalt complexes bearing 2,9-diimino-1,10-phenanthrolines showed low activity for ethylene reactivity [11], it was assumed that the additional imino group would coordinate with active sites to prevent the coordination of ethylene. The direct evidence was provided by our recent results, the iron complexes ligated by 2-imino-1,10-phenanthrolines indeed showed very high activities for ethylene oligomerization and polymerization [12], while the contributing works by the Solan group [13] and ours [14] revealed their cobalt analogues as catalysts with good activity along with the highly active nickel catalysts [15].

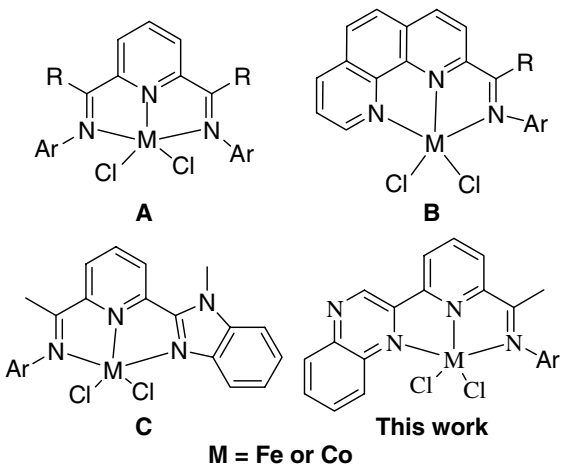

Comparing the models of highly active catalysts of iron and cobalt complexes with the backbones of 2,6-bis(imino)-pyridines (**A**) [6,7] and 2-imino-1,10-phenanthrolines (**B**) [12–14], the heteroatomic compounds as flexible ligands would be interesting on the basis of pyridine derivatives. Extensively, the iron and cobalt complexes bearing 2-(2-benzimidazole)-6-(1-aryliminoethyl)pyridines (**C**) also showed highly ethylene catalytic activities [16]. In addition, the 2-ethylcarboxylate-6-iminopyridyl iron and cobalt complexes equally exhibited considerable catalytic activity for ethylene oligomerization and polymerization [17]. Recently bimetallic complexes based on 2-methyl-2,4-bis(6-iminopyridin-2-yl)-1*H*-1,5-benzodiazepines showed good activity for ethylene oligomerization and polymerization with high selectivity for α-olefins and vinyl-type polyethylene waxes [18]. Inspired by these good results, we embarked on the preparation of (6-(quinoxalin-2-yl)pyridine-2-yl)ethylidene)benzenamines [2-quinoxalinyl-6-iminopyridines] and their metal complexes. The desired ligand substance, 1-(6-(quinoxalin-2-yl)pyridin-2-yl)ethanone, however, could not be available neither commercially nor by standing synthetic methodology. Therefore the suitable synthetic procedure for this compound was developed, subsequently the condensation reaction with substituted anilines gave *N*-(1-(6-(quinoxalin-2-yl)pyridine-2-yl)ethylidene)benzenamines [2-quinoxalinyl-6-iminopyridines] for their iron and cobalt complexes. The organic compounds and their iron and cobalt complexes were fully characterized, and their structural features were discussed in detail. Activated with methylaluminoxane (MAO), the iron complexes exhibited good activities for ethylene oligomerization and polymerization; meanwhile their cobalt analogues showed moderate catalytic activity with modified methylaluminoxane (MMAO). Herein, the synthesis and characterization of *N*-(1-(6-(quinoxalin-2-yl)pyridine-2-yl)ethylidene)benzenamines and their iron and cobalt complexes are reported and discussed along with their catalytic behaviors toward ethylene oligomerization and polymerization.

2. Results and discussion

2.1. Synthesis and characterization

In order to design new iron and cobalt catalysts model, the synthesis of organic compounds as the hybrid of functional groups will be mainly challenged. With the purpose of synthesizing *N*-(1-(6-(quinoxalin-2-yl)pyridine-2-yl)ethylidene)benzenamines, the basic substance 1-(6-(quinoxalin-3-yl)pyridine-2-yl)ethanone, however, is not available with synthetic protocol in the literature. Though the reaction of arylethanone with *o*-phenylenediamine to produce the aryl-quinoxaline derivatives was investigated in our group [19], such reaction pathway cannot be extended to the reaction of 6-acetylpyridine-2-carboxylate [17,20] with

o-phenylenediamine for ethyl 6-(quinoxalin-2-yl)picolinate. Instead, it produced a domain 7-membered cyclic compound as in the reported case of 1,5-benzodiazepine derivatives [19a,22]. The general synthetic method of quinoxalines consists of the condensation reactions of ethane-1,2-diol with *o*-phenylenediamine [21], the obstacle is that no suitable starting material which bears appropriate functional groups is available. Therefore, the need to explore new synthetic methodology for the target compound of 1-(6-(quinoxalin-3-yl)pyridine-2-yl)ethanone, on the base of new compound 6-acetylpyridine-2-carboxylate, is inevitable [17,20].

According to the plausible mechanism in forming 6-membered or 7-membered cyclic compounds by the reactions of arylethanones with *o*-phenylenediamines [19a], the competition of the intra- or inter-molecular coupling reactions after amine-ketone condensation is a key issue to be addressed. The intramolecular coupling reaction obviously favored must be to form 6-membered cyclic compounds, the quinoxalinyl group. In order to achieve this, the acetyl group was selectively activated through the bromination of its methyl end. For the bromination [23], with one equivalent of bromine which is often used, the ethyl 6-(2-bromoacetyl)pyridine-2-carboxylate was obtained in 60% yield, however, in 89% yield with two equivalent moles of bromine. In the following, the solvent mixture of methanol and pyridine was used in the reaction of ethyl 6-(2-bromoacetyl)pyridine-2-carboxylate with *o*-phenylenediamine, based on the consideration of the common solvent methanol and pyridine used to neutralize the formed acidic hydrogen bromide. The ethyl 6-(quinoxalin-3-yl)pyridine-2-carboxylate was obtained as white solid in 52% isolated yield . Furthermore, the conversion of carbethoxy group into acetyl group affords the white solid 1-(6-(quinoxalin-3-yl)pyridine-2-yl)ethanone in 65% isolated yield. With 6-acetylpyridine-2-carboxylate as a starting material, the synthesis of 1-(6-(quinoxalin-3-yl)pyridine-2-yl)ethanone was finally achieved and the synthetic procedure is illustrated in Scheme 1.

The routine synthetic method for 2-quinoxalinyl-6-iminopyridines (**L1**–**L7**) is the condensation of 1-(6-(quinoxalin-3-yl)pyridine-2-yl)ethanone with corresponding anilines

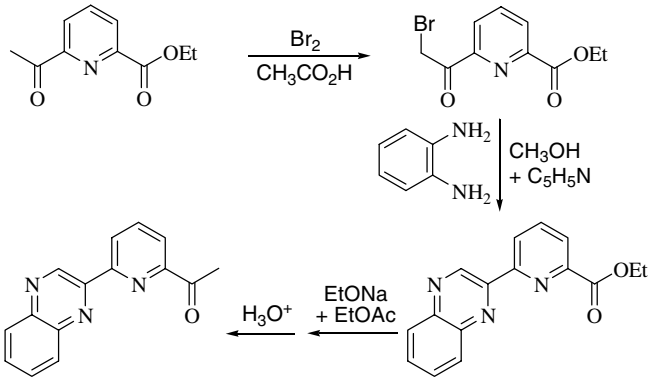

Scheme 1. Synthesis of 1-(6-(quinoxalin-2-yl)pyridin-2-yl)ethanone.

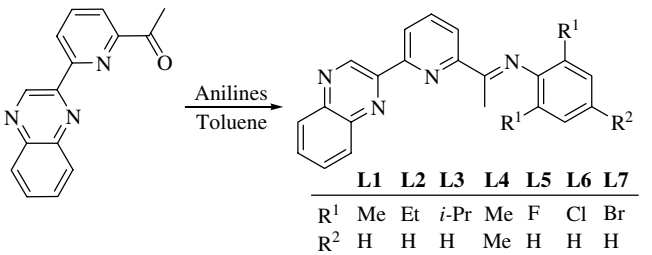

	L1	L2	L3	L4	L5	L6	L7
R^1	Me	Et	*i*-Pr	Me	F	Cl	Br
R^2	H	H	H	Me	H	H	H

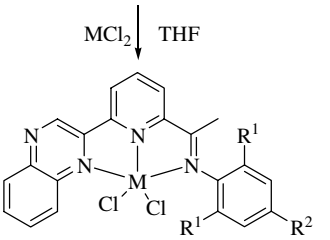

	1	2	3	4	5	6	7	8	9	10	11	12	13	14
M	Fe	Fe	Fe	Fe	Fe	Fe	Fe	Co	Co	Co	Co	Co	Co	Co
R^1	Me	Et	*i*-Pr	Me	F	Cl	Br	Me	Et	*i*-Pr	Me	F	Cl	Br
R^2	H	H	H	Me	H	H	H	H	H	H	Me	H	H	H

Scheme 2. Synthesis of 2-quinoxalinyl-6-iminopyridines and their iron and cobalt complexes.

(Scheme 2). For the synthesis of 2-quinoxalinyl-6-iminopyridines, compounds **L1**–**L5** were easily synthesized in acceptable yields in the presence of catalytic amount of *p*-toluenesulfonic acid. However, it is necessary to use excessive amount of the corresponding anilines (1.2 equiv.) and tetraethyl silicate as the water absorbent in synthesizing compounds **L6** and **L7** with relatively lower yields. All the synthesized 2-quinoxalinyl-6-iminopyridines were obtained as yellow powders and confirmed by IR, ^{1}H NMR, ^{13}C NMR and elemental analysis. Moreover, the single crystals of **L1** and **L4** suitable for X-ray diffraction analysis were grown by slow evaporation of their hexane–EtOAc (8:1) solution.

Their iron complexes (**1**–**7**) were obtained in good yields as blue solid by the reaction of $FeCl_2 \cdot 4H_2O$ and one equivalent 2-quinoxalinyl-6-iminopyridines in freshly distilled tetrahydrofuran (THF) at room temperature; while their cobalt complexes (**8**–**14**) were obtained in good yields (69–78%) as green solids by the same procedure (Scheme 2). All the complexes are stable in solid states, but iron complexes are unstable in their solution due to the oxidation of Fe(II) into Fe(III) which is indicated by the color change of the solution from blue to yellow when exposed to air. These complexes were characterized by elemental analysis and IR spectroscopy. For the iron complexes, compared with the IR absorptions of C=N group of free ligands in the range of 1637–1651 cm^{-1} with strong intensities, the C=N stretching frequencies of complexes were shown between 1611 and 1634 cm^{-1} with weak intensities confirming the coordination interaction between ligands and iron center. Similar to the iron complexes, all cobalt complexes also showed lower C=N stretching frequencies along with decreased peak intensity in contrast to their corresponding free ligands. These iron(II) and cobalt(II)

complexes are paramagnetic, and magnetic susceptibilities were determined by Evans' NMR method [24]. The magnetic moments for these complexes suggest the presence of high spin ($S = 5/2$) configurations and lower field strength of the title ligands. However, magnetic susceptibilities of complexes **2** and **9** were not obtained due to their lower solubility. In addition, the single crystals of **1**, **4**, **10** and **13** suitable for X-ray diffraction analysis were obtained and their unambiguous molecular structures were determined.

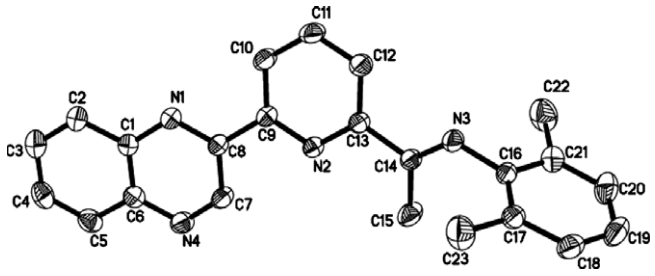

Fig. 1. Molecular structure of **L1**. Thermal ellipsoids are shown at 30% probability. Hydrogen atoms have been omitted for clarity.

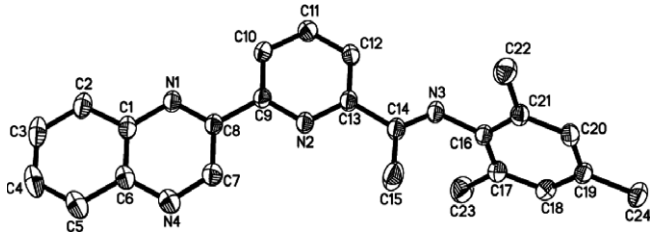

Fig. 2. Molecular structure of **L4**. Thermal ellipsoids are shown at 30% probability. Hydrogen atoms have been omitted for clarity.

The crystal structures of **L1** and **L4** were shown in Figs. 1 and 2. According to the molecular structure, the quinoxalinyl group and substituted phenyl group were stretched far away for releasing the steric constraints and the imine group is in the *E* formation with typical C=N double bond in **L1** (1.267(3) Å) and **L4** (1.2652(2) Å). The *N*-aryl ring forms a dihedral angle of 68.5° in **L1** and 106.0° in **L4** with the pyridyl ring, while the quinoxalinyl group is approximately coplanar with pyridyl ring, and forms a dihedral angle of 11.3° and 5.0°, respectively. The quinoxalinyl group is located as the *anti*-form to pyridyl ring in its solid, and the single bond nature of C(8)–C(9) indicates that quinoxalinyl group may rotate around the C(8)–C(9) bond to interconvert *syn*- and *anti*-forms. Their selected bond lengths and angles are listed in Table 1.

To confirm the molecular structures of these metal complexes, the conclusive results could be obtained by single crystal X-ray diffraction analysis. Single crystals of complexes **1**, **4**, **10**, **13** suitable for X-ray diffraction analysis

Table 1
Selected bond lengths (Å) and angles (°) for **L1**, **L4**, **1**, **4**, **10** and **13**

	L1	**L4**	**1**	**4**	**10**	**13**
Bond lengths (Å)						
M–N(1)	–	–	2.276(4)	2.286(5)	2.287(3)	2.191(2)
M–N(2)	–	–	2.122(4)	2.125(5)	2.063(3)	2.021(2)
M–N(3)	–	–	2.234(4)	2.227(5)	2.221(3)	2.220(2)
M–Cl(1)	–	–	2.2827(2)	2.2863(2)	2.2694(1)	2.2249(9)
M–Cl(2)	–	–	2.2925(2)	2.3059(2)	2.2581(1)	2.2773(8)
N(1)–C(8)	1.320(3)	1.3182(2)	1.332(6)	1.327(7)	1.318(4)	1.326(3)
N(2)–C(9)	1.348(3)	1.3444(2)	1.329(6)	1.332(7)	1.350(4)	1.345(3)
N(2)–C(13)	1.338(3)	1.3397(2)	1.342(6)	1.345(7)	1.339(4)	1.341(3)
N(3)–C(14)	1.267(3)	1.2652(2)	1.273(6)	1.280(7)	1.280(4)	1.284(3)
N(3)–C(16)	1.425(3)	1.4230(2)	1.448(6)	1.444(7)	1.451(4)	1.432(3)
C(8)–C(9)	1.474(3)	1.4818(2)	1.465(7)	1.469(8)	1.475(5)	1.482(3)
C(13)–C(14)	1.498(3)	1.4959(2)	1.487(6)	1.492(8)	1.493(5)	1.497(4)
C(14)–C(15)	1.507(3)	1.498(2)	1.502(7)	1.490(8)	1.501(5)	1.493(4)
Bond angles (°)						
N(1)–C(8)–C(9)	117.47(2)	117.77(1)	116.2(4)	116.0(5)	117.0(3)	116.2(2)
N(2)–C(9)–C(8)	116.95(2)	116.48(1)	114.6(4)	115.5(5)	114.1(3)	113.6(2)
N(2)–C(13)–C(14)	116.80(2)	117.18(1)	114.5(4)	115.3(5)	114.5(3)	113.9(2)
N(3)–C(14)–C(13)	117.21(2)	116.96(1)	116.2(4)	114.8(5)	116.2(3)	115.7(2)
C(14)–N(3)–C(16)	122.28(2)	122.46(1)	118.2(4)	120.2(5)	118.9(3)	121.2(2)
N(1)–M–N(2)	–	–	72.65(1)	72.97(2)	74.06(1)	76.67(8)
N(1)–M–N(3)	–	–	146.10(1)	145.84(2)	147.95(1)	151.70(8)
N(2)–M–N(3)	–	–	73.45(1)	73.45(2)	75.12(1)	75.51(8)
N(1)–M–Cl(1)	–	–	96.46(1)	94.78(1)	93.04(8)	93.99(6)
N(1)–M–Cl(2)	–	–	98.05(1)	98.80(1)	100.72(8)	91.33(6)
N(2)–M–Cl(1)	–	–	124.13(1)	117.47(1)	109.54(8)	127.91(7)
N(2)–M–Cl(2)	–	–	127.34(1)	132.52(1)	140.31(9)	107.06(6)
N(3)–M–Cl(1)	–	–	102.42(1)	106.06(1)	105.35(8)	98.96(6)
N(3)–M–Cl(2)	–	–	102.33(1)	99.18(1)	97.34(8)	101.64(6)
Cl(1)–M–Cl(2)	–	–	108.24(6)	109.70(6)	110.03(5)	124.50(4)

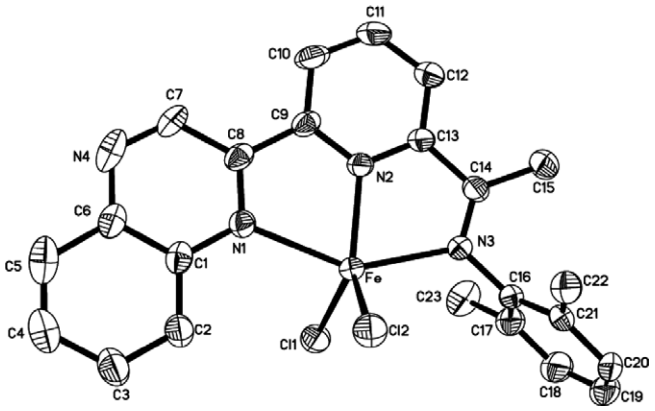

Fig. 3. Molecular structure of complex **1**. Thermal ellipsoids are shown at 30% probability. Hydrogen atoms and one diethyl ether molecule have been omitted for clarity.

were obtained by slow diffusion of diethyl ether into their methanol solutions. The crystal structure of iron complex **1** revealed the coordinated geometry around the metal center as a distorted trigonal-bipyramidal with the pyridyl nitrogen atom and the two chlorine atoms forming an equatorial plane (Fig. 3). The deviation of the iron center from the equatorial plane is 0.0701 Å. The two nitrogen atoms (N1 and N3) occupy the axial coordination sites with the bond angle of 146.10(1)° for N1–Fe–N3 and the dihedral angle between the equatorial plane and the axial plane is 89.4°. The phenyl ring lies almost perpendicular to the plane formed by the coordinated nitrogen atoms (90.1°), which is similar to the 2,6-bis(imino)pyridyl iron(II) complexes [6,7] 2-imino-1,10-phenanthrolinyl iron(II) complexes [12] and 2-(2-benzimidazole)-6-(1-arylimino-ethyl)pyridyl iron(II) complexes [16]. Furthermore, the two Fe–Cl bond lengths show a slight difference between the Fe–Cl1 (2.2827(2) Å) and Fe–Cl2 (2.2925(2) Å). The difference usually appears in the tridentate N^N^N iron(II) complexes because of apical elongation in the square-pyramidal complex [25]. The Fe–N2(pyridyl) (2.122(4) Å) bond is shorter than the Fe–N3(imino) (2.234(4) Å) bond and the Fe–N1(quinoxalinyl) (2.276(4) Å) bond, similar to the 2,6-bis(imino)pyridyl iron(II) complexes [6,7] and 2-imino-1,10-phenanthrolinyl iron(II) complexes [12]. Furthermore, the imino N3–C14 bond in **1** displays clear double-bond character (1.273(6) Å) and is slightly (0.0063 Å) longer than that in the free ligand **L1**.

The molecular structure of complex **4** is shown in Fig. 4 with its selected bond lengths and angles in Table 1. It has a similar coordinate geometry with **1**. The observed similarities include the identical bond lengths and angles and the shortest Fe–N2(pyridine) bond (2.125(5) Å) among the three Fe–N bonds. Also the equatorial plane and phenyl plane is nearly perpendicular to the quinoxalinyl ring. However, there are some slight differences between the two structures. The iron atom deviates by 0.1715 Å from the coordinated plane, which is much larger than that in complex **1**.

Complex **10** with 2,6-diisopropylphenyl and complex **13** with 2,6-dichlorophenyl almost have similar structural characters, as shown in Figs. 5 and 6 (their bond lengths and angles are listed in Table 1). The nitrogen atom of pyridine and two chlorides form the equatorial plane. The cobalt atom deviates this plane by 0.0439 Å in **10** and 0.0904 Å in **13**. The equatorial planes of these two

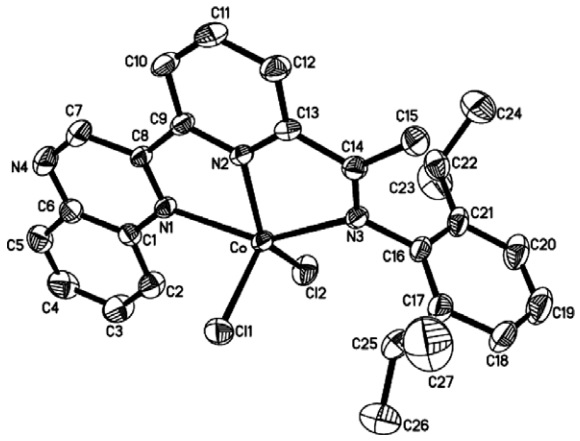

Fig. 5. Molecular structure of complex **10**. Thermal ellipsoids are shown at 30% probability. Hydrogen atoms have been omitted for clarity.

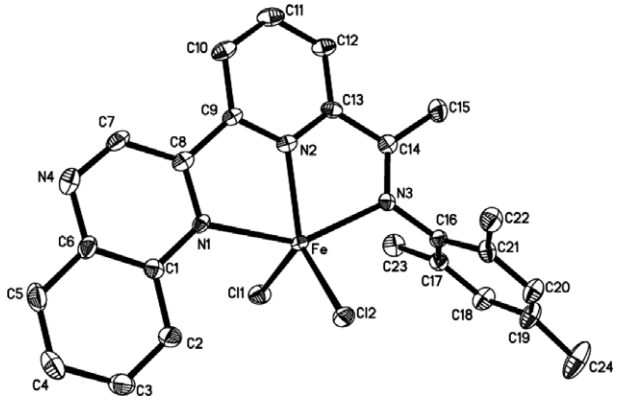

Fig. 4. Molecular structure of complex **4**. Thermal ellipsoids are shown at 30% probability. Hydrogen atoms and diethyl ether molecule have been omitted for clarity.

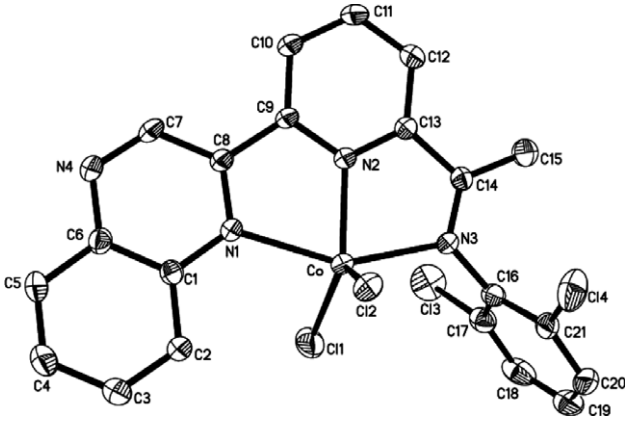

Fig. 6. Molecular structure of complex **13**. Thermal ellipsoids are shown at 30% probability. Hydrogen atoms have been omitted for clarity.

complexes are nearly perpendicular to the quinoxalinyl ring, with dihedral angles of 86.5° in **10** and 91.1° in **13**. The equatorial Co–N bonds are relatively shorter than their axial Co–N bonds. All these characters are similar with the reported N^N^N tridentate cobalt complexes [6,7,13,16]. Furthermore, the imino N3–C14 bond reveals clear double-bond character (1.280(4) Å in **10** and 1.284(3) Å in **13**). Due to the different substituent on the phenyl ring, these two complexes show different equatorial angles especially for the Cl1–Co–Cl2 bond angles (110.03(5)° in **10** and 124.50(4)° in **13**). A slight difference (0.011 Å) between the Fe–Cl1 and Fe–Cl2 bonds is observed, however, the difference(0.052 Å) is much larger in **13**. In complex **10**, the pyridine plane and quinoxalinyl ring are almost coplanar, with a dihedral angle of 1.7°. In complex **13**, the quinoxalinyl ring deviates the pyridine plane with a dihedral angle of 15.2°.

2.2. Ethylene oligomerization and polymerization

The catalytic reactivity of the title N^N^N tridentate metal complexes were generally investigated in the presence of various cocatalysts such as MAO, MMAO or Et_2AlCl. Considering significant differences of catalytic behaviors between iron and cobalt complexes, the results and discussions are separated into two individual parts for the iron and cobalt systems.

2.2.1. Ethylene reactivity of iron complexes

2.2.1.1. The selection of cocatalyst. Various cocatalysts such as Et_2AlCl, MMAO and MAO were used to activate complex **4** for ethylene reactivity at room temperature and ambient pressure (Table 2). The iron catalytic system containing MAO showed the highest activities for ethylene oligomerization, and the butenes were observed as the major products. Beyond that, only butenes were formed in the catalytic system with Et_2AlCl. Though, the system with MMAO showed considerable catalytic activities, the analyses of oligomers produced were somehow affected due to the isobutyl group in MMAO. Therefore, further catalytic studies were performed by the activation with MAO, and the analyses of the obtained oligomers were carried out by GC and GC–MS.

2.2.1.2. Ethylene reactivity in the presence of MAO. The effects of Al/Fe molar ratio on catalytic activities of ethylene oligomerization were investigated with complex **4** in order to find the suitable molar ratio for better activity. With the Al/Fe ratio enhanced from 200 to 1500, the activity of **4** was initially increased and then decreased with optimum catalytic activity at Al/Fe molar ratio of 1000. These observed phenomena are often explained by the fact that enough amount of MAO is necessary in activating precursors in order to obtain more active species, however, the plausible remaining trimethylaluminium in MAO may deactivate the active species [8d]. The reaction temperature should also be considered because the ethylene reactivity is a highly exothermic reaction and the catalytic activity will therefore be varied at different temperatures. To understand such influence, the catalytic system of **4** with 1000 equiv. MAO at 1 atm was investigated with changing reaction temperature (entries 3, 5–7 in Table 3). Elevating the reaction temperature from 0 to 60 °C, the catalytic system showed highest activity at 20 °C; and solubility of ethylene and stability of active species would be both considered [7b,7d]. Moreover, the oligomers distribution became narrower along with the decreased catalytic reactivity. The proportion of C_4 and other short-chain oligomers were greatly increased at higher temperature because of the faster β-hydrogen elimination than ethylene propagation.

Different substituents on the imino-*N* aryl ring could have some influences on their catalytic performance. For complexes **1**–**3**, their activities are in same order with comparable values (entries 1–3 and 8–10 in Table 4). In the catalytic systems of complexes **5**–**7** containing 2,6-dihalosubstituted ligands, the bulkier substituents at the *ortho*-positions of the imino-*N* aryl ring resulted in lower catalytic activities (**6**, **5** > **7**, entries 11–13 in Table 4). This phenomenon could be rooted back to the combination of bulky and electronic effects of ligands, the covalent radius are F, 0.72, Cl, 0.99 and Br, 1.14 Å, while the electronegativties of fluorine, chlorine and bromine atom are 4.0, 3.0 and 2.8, respectively. The complexes with electron-withdrawing groups showed similar catalytic reactivity as their analogues with electron-donating groups, but the narrower distribution of oligomers with shorter chains was observed because of the faster β-hydrogen elimination than ethylene propagation. Interestingly, the substituent at the *para*-position of the aryl ring had an obvious influence on the reactivity and distribution of oligomers. In contrast to

Table 2
Selection of the suitable cocatalyst based on **4**

Entry	Cocatalyst	Al/Fe	Oligomer activity[a]	Oligomer distribution				
				C_4	C_6	C_8	C_{10}	$\sum C_{\geqslant 12}$
1	Et_2AlCl	200	0.01	100	–	–	–	–
2	MMAO	1000	5.07	80.7	8.3	3.5	1.7	5.8
3	MAO	1000	7.13	71.0	10.9	2.0	1.9	14.2

Reaction condition: 5 μmol Fe; 30 mL toluene. 1 atm of ethylene; 20 °C; 30 min.
[a] 10^5 g mol Fe^{-1} h^{-1}.

Table 3
Oligomerization of ethylene with **4**/MAO

Entry	Al/Fe	*T*/°C	Oligomer activity[a]	Oligomer distribution				
				C_4	C_6	C_8	C_{10}	$\sum C_{\geqslant 12}$
1	200	20	0.52	95.3	4.7	–	–	–
2	500	20	0.63	95.8	4.2	–	–	–
3	1000	20	7.13	71.0	10.9	2.0	1.9	14.2
4	1500	20	2.69	84.7	6.3	3.3	1.0	4.7
5	1000	0	0.77	90.1	5.0	3.7	0.3	0.9
6	1000	40	1.04	80.0	6.5	6.0	1.8	5.7
7	1000	60	0.13	92.4	7.6	–	–	–

Reaction condition: 5 μmol Fe; 30 mL toluene; 1 atm of ethylene; 30 min.
[a] 10^5 g mol Fe^{-1} h^{-1}.

Table 4
Oligomerization of ethylene with **1**–**7**/MAO

Entry	Complex	*T*/min	Oligomer activity[a]	Oligomer distribution[b]				
				C_4	C_6	C_8	C_{10}	$\sum C_{\geqslant 12}$
1	**1**	10	4.50	91.4	6.7	0.6	0.2	1.1
2	**2**	10	5.32	96.1	3.4	0.3	0.1	0.1
3	**3**	10	4.12	98.6	1.4	–	–	–
4	**4**	10	12.0	84.8	9.2	1.5	1.1	3.4
5	**5**	10	4.62	87.4	12.2	0.4	–	
6	**6**	10	5.07	96.4	3.6	–	–	–
7	**7**	10	1.72	94.6	5.4	–	–	–
8	**1**	30	1.53	90.7	7.4	0.6	0.2	1.1
9	**2**	30	2.66	95.6	4.0	0.2	0.1	0.1
10	**3**	30	1.69	98.8	1.2	–	–	–
11	**4**	30	7.13	71.0	10.9	2.0	1.9	14.2
12	**5**	30	2.20	86.2	13.6	0.2	–	–
13	**6**	30	2.55	95.6	4.4	–	–	–
14	**7**	30	1.39	94.4	5.6	–	–	–
15	**7**	5	1.65	94.0	6.0	–	–	–
16	**7**	10	1.72	94.6	5.4	–	–	–
17	**7**	15	1.78	94.8	5.2	–	–	–
18	**7**	20	1.62	94.3	5.7	–	–	–
19	**7**	25	1.51	94.5	5.5	–	–	–

Reaction condition: 5 μmol Fe; cocat.: MAO; Al/Fe = 1000; 1 atm ethylene; 20 °C; 30 mL toluene.
[a] 10^5 g mol Fe^{-1} h^{-1}.
[b] Determined by GC.

1/MAO system, **4**/MAO with 2,4,6-trimethylphenyl group showed four times higher catalytic activity with greatly increased long-chain oligomers (entries 1, 4 and 8, 11 in Table 4).

Ethylene reactivity with different reaction times was also investigated and the results were summarized in Table 4. Accordingly the catalytic activity within 10 min was higher than that obtained within 30 min, in which sharp decrease was clearly observed. It could be imagined that the active species were not stable and rendered the activity remarkably reduced within 30 min (entries 1–7 in Table 4). To understand such influence, the catalytic system of **7** was investigated in detail with changing reaction time (entries 14–19 in Table 4). When the reaction time was increased from 5 to 15 min, the activity was slowly enhanced, and then decreased with longer time which indicated that the active species performed best within 15 min and then deactivated because of their instability.

It is well known that elevated ethylene pressure promotes higher activities, this phenomenon was also observed with the iron catalytic system. The results of ethylene reactivity at 10 atm were summarized in Table 5.

Comparing Table 5 with Table 4, both activity and contents of longer-chain oligomers increased at 10 atm. In the cases of **1**, **3** and **4** catalytic systems, the polyethylene waxes were collected to prove good polymerization activity; especially for **4**/MAO system, its reactivity for oligomers and polymers were both enhanced sharply at 10 atm pressure. According to Table 5 (entries 1–3), the oligomerization activity was decreased sharply with large bulkier substituents on the *N*-aryl ring. Besides, similar to the catalytic system at 1 atm, the substituent at the 4-position of the aryl ring also showed an important influence on the activity and **4**/MAO system displayed the highest reactivity. From the IR spectra, the obtained PE samples demonstrated the PE's linear characteristics and the presence of the vinyl end groups. Moreover, the NMR spectra confirm their vinyl-type olefin waxes.

Table 5
Ethylene reactivity with **1**–**7**/MAO at 10 atm

Entry	Complex	Activity[a]		Oligomer distribution				
		Polymer	Oligomer	C_4	C_6	C_8	C_{10}	$\sum C_{\geqslant 12}$
1	**1**	3.86	7.94	87.7	5.9	2.6	0.5	3.3
2	**2**	–	3.71	91.6	4.0	3.2	0.3	0.9
3	**3**	4.27	0.78	94.9	1.9	1.9	0.3	1.0
4	**4**	8.56	22.4	74.5	7.3	2.9	2.0	13.3
5	**5**	–	2.40	95.4	3.2	1.4	–	–
6	**6**	–	3.91	94.5	3.9	0.7	0.3	0.6
7	**7**	–	4.65	92.2	3.9	3.0	0.3	0.6

Reaction condition: 5 μmol Fe; cocat.: MAO; Al/Fe = 1000; 10 atm ethylene; 20 °C; 30 min; 100 mL toluene.
[a] 10^5 g mol Fe^{-1} h^{-1}.

2.2.2. Ethylene reactivity by cobalt complexes

Similar to the above iron complexes, all cobalt(II) analogues displayed considerable catalytic activities for ethylene oligomerization. Though catalytic systems with MAO or Et_2AlCl also demonstrated catalytic activities (entries 1 and 3 in Table 6), the catalytic system with MMAO showed better result; therefore further investigation of cobalt catalysts was carried out with MMAO as cocatalyst.

Various results of ethylene oligomerization by cobalt complexes at ambient pressure were collected in Table 6. The catalytic activity of the cobalt complexes was also remarkably influenced by different substituents on the aryl rings. Similar to the iron complexes, cobalt complex **9** performed better reactivity than **8** and **10**. In the catalytic systems of complexes **12**–**14** containing 2,6-dihalosubstituents (entries 5–7 in Table 7), their activities remained in the order of bromo- > chloro- > fluoro-, in which the bulkier substituents at the *ortho*-positions of the imino-*N* aryl ring resulted in higher catalytic activities. Additionally the substituent at the *para*-position of the aryl ring had no obvious influence on the reactivity which is different with the iron analogues. Another notable difference between the cobalt and iron complexes is that cobalt analogues produced more oligomers with shorter-chains because of the faster β-hydrogen elimination.

Table 6
Influences of cocatalyst on activity of complex **8**

Entry	Co-cat.	Al/Co	Activity[a]	Oligomer distribution		
			Oligomer	C_4	C_6	$\sum C_{\geqslant 8}$
1	Et_2AlCl	200	0.1	100	–	–
2	MMAO	1000	10.5	96.5	1.6	1.9
3	MAO	1000	4.1	88.1	2.9	9.0

Reaction condition: 5 μmol Co; 30 mL toluene. 1 atm ethylene; 20 °C; 30 min.
[a] 10^4 g mol Co^{-1} h^{-1}.

Table 7
Oligomerization of ethylene with **8**–**14**/MMAO

Entry	Complex	Al/Co	T/°C	Activity[a]	Oligomer distribution[b]		
				Oligomer	C_4	C_6	$\sum C_{\geqslant 8}$
1	**8**	1000	20	10.5	96.5	1.6	1.9
2	**9**	1000	20	14.3	98.5	1.5	–
3	**10**	1000	20	10.6	98.9	1.1	–
4	**11**	1000	20	10.8	96.6	1.4	2.0
5	**12**	1000	20	7.7	96.7	3.3	–
6	**13**	1000	20	16.1	97.8	2.2	–
7	**14**	1000	20	16.7	96.4	3.6	–
8	**11**	200	20	2.2	98.4	1.6	–
9	**11**	500	20	7.8	94.1	1.3	4.6
10	**11**	1500	20	13.0	96.1	1.1	2.8
11	**11**	2000	20	16.1	97.4	1.0	1.6
12	**11**	2500	20	15.4	97.4	0.9	1.7
13	**11**	1000	0	13.2	97.0	1.6	1.4
14	**11**	1000	40	3.4	96.9	0.8	2.3
15	**11**	1000	60	6.3	100	–	–

Reaction condition: 5 μmol Co; cocat.: MMAO; 1 atm ethylene; 0.5 h; 20 °C; 30 mL toluene.
[a] 10^4 g mol Co^{-1} h^{-1}.
[b] Determined by GC.

The catalytic activity of cobalt complexes was also affected by varying the reaction parameters, and complex **11** was used as an example. When the Al/Co molar ratio was enhanced from 200 to 2500, the catalytic activities initially increased and then decreased with optimum activity at the Al/Co molar ratio of 2000 (entries 4, 8–12 in Table 7). Notably, the catalytic activity increased sharply with broader oligomers distribution when the Al/Co molar ratio was increased from 200 to 500, which may be attributed to MMAO scavenged adventitious water and impurities in the solvent at the Al/Fe ratio of 200 a such, the cobalt complex required more cocatalyst to be active. When the Al/Co molar ratio was increased to 2000, the activity was slowly enhanced, and then decreased at Al/Co molar ratio of 2500 which could be traced to the increasing amount of isobutyl group, and the generated species hinder the insertion of ethylene due to steric bulkiness [26]. Elevating the reaction temperature from 0 to 60 °C resulted in decreasing catalytic activity (entries 4, 13–15 in Table 7), which might be caused by instability of the active species or lower concentration of ethylene at high temperature. Only butenes were produced with the reaction temperature of 60 °C.

Ethylene reactivity by cobalt complexes **8**–**14** was studied at 10 atm of ethylene with MMAO at Al/Co ratio of 1000. However, their catalytic activities were not significantly enhanced except for **11**. In **11**/MMAO system at 10 atm, a large amount of polyethylene waxes was produced with the activity of 4.04×10^5 g mol^{-1} (Co) h^{-1} and the contents of longer-chain oligomers were also increased. The polyethylene waxes were confirmed possessing linear characteristics with the presence of the vinyl end groups. The effect of substituents on ethylene reactivity at 10 atm of ethylene followed the same trend with those obtained at 1 atm.

2.3. Conclusions

The new N^N^N ligand 2-imino-6-(quinoxalin-3-yl)pyridines were prepared and reacted with iron and cobalt chlorides to form the title complexes. Sharing the similar framework with complexes containing 2,6-bis(imino)pyridines [6,7] or 2-imino-1,10-phenanthrolines [12–14], and 2-(2-benzoimidazole)-6-(1-aryliminoethyl)-pyridines [16], the iron complexes exhibited good activities for ethylene oligomerization and polymerization in the presence of MAO, and a large amount of α-linear polyethylene waxes were produced at 10 atm ethylene pressure. The higher activities were obtained at lower reaction temperature because of the thermal instability for active species. The cobalt complexes exhibited moderate to good activities for ethylene reactivity in the presence of MMAO.

3. Experimental

All synthetic manipulations were carried out under nitrogen atmosphere using standard Schlenk and cannula techniques. NMR were recorded on Bruker DMX-300 spectrometer, with TMS as the internal standard. Elemental analyses were performed on a Flash EA 1112 microanalyzer. IR spectra were obtained as KBr pellets on a Perkin–Elmer FTIR 2000 spectrometer. Melting points (Mp) were determined with a digital electrothermal apparatus without further correction. Magnetic susceptibilities were determined by Evans' NMR method [24] in methanol-d_4/cyclohexane (97:3 v/v) solution at room temperature. GC analyses were performed with a VARIAN CP-3800 Strumentazione gas chromatograph equipped with a flame ionization detector and a 30 m (0.2 mm i.d., 0.25 μm film thickness) CP-Sil 5 CB column. GC–MS analyses were performed with HP 5890 SERIES II and HP 5971 SERIES mass detectors. THF and toluene were refluxed over as sodium benzophenone and distilled under nitrogen, while other solvents were refluxed over an appropriate drying agent and distilled under nitrogen prior to use. Methylaluminoxane (MAO, 1.46 M solution in toluene) and modified methylaluminoxane (MMAO, 1.93 M in heptane, 3A) were purchased from Akzo Nobel Corp. Diethylaluminum chloride (Et_2AlCl, 1.7 M in toluene) was purchased from Acros Chemicals. All other chemicals were purchased and used without further purification, except for ethyl 6-acetylpyridine-2-carboxylate prepared with an established procedure [17,20]. The boiling range of petroleum ether is 30–60 and brand of silica gel is 200–300 mesh.

3.1. Synthesis of 1-(6-(quinoxalin-2-yl)pyridine-2-yl)ethanone

3.1.1. Ethyl 6-(2-bromoacetyl)pyridine-2-carboxylate

The solution of bromine (1.06 mL, 0.02 mol) in acetic acid (10 mL) was added dropwise to a solution of ethyl

6-acetylpyridine-2-carboxylate (1.93 g, 0.01 mol) and several drops of hydrobromic acid in acetic acid (20 mL), the mixture was then stirred at room temperature for 3–4 h. The solvents were evaporated and the residue was eluted on column chromatography [silica gel; eluting reagent light petroleum–EtOAc (6:1)]. The desired product was obtained as white solid with 89% isolated yield (2.42 g). Mp: 98–99 °C. IR (KBr, cm^{-1}): 1722 (s, $\nu_{C=O}$), 1586, 1320, 1256, 1154 (s, ν_{C-O-C}), 1007, 993, 762, 665, 632. ^1H NMR (300 MHz, $CDCl_3$, δ): 8.35 (d, 1H, $J = 7.9$ Hz, *Py*–H), 8.26 (d, 1H, $J = 7.70$ Hz, *Py*–H), 8.05 (t, $J = 7.56$ Hz, 1H, *Py*–H), 4.99 (s, 2H, CH_2Br), 4.51 (m, 2H, –OCH_2–), 1.47 (t, 3H, $J = 7.70$ Hz, CH_3). ^{13}C NMR (75.45 MHz, $CDCl_3$, δ): 191.8, 164.1, 151.2, 147.9, 138.3, 128.7, 125.2, 62.0, 32.6, 14.2. Anal. Calc. for $C_{10}H_{10}BrNO_3$: N, 5.15; C, 44.14; H, 3.70. Found: N, 4.96; C, 44.10; H, 3.84%.

3.1.2. Ethyl 6-(quinoxalin-2-yl)pyridine-2-carboxylate

Ethyl 6-(2-bromoacetyl)pyridine-2-carboxylate (1.87 g, 0.006 mol) was added to the solution of 1,2-phenylene diamine (0.65 g, 0.006 mol) in methanol (20 mL) and pyridine (5 mL). The mixture was stirred and refluxed for 3 h. The solvents were evaporated and the residue was eluted on column chromatography [silica gel, eluting reagent: light petroleum–EtOAc (5:1)] to obtain the product as white solid in 52% isolated yield (0.87 g). Mp: 137–138 °C. IR (KBr, cm^{-1}): 1714 (s, $\nu_{C=O}$), 1588, 1568, 1554, 1310, 1247, 1148 (s, ν_{C-O-C}), 771, 405. ^1H NMR (300 MHz, $CDCl_3$, δ): 10.11 (s, 1H, *o*-quinoxalin-H), 8.81 (d, 1H, $J = 7.7$ Hz, *Py*–H), 8.25 (d, 1H, $J = 7.95$ Hz, *Py*–H), 8.20 (m, 2H, quinoxalin-H), 8.07 (t, 1H, $J = 7.50$ Hz, *Py*–H), 7.83 (m, 2H, quinoxalin-H), 4.55 (m, 2H, OCH_2), 1.52 (t, 3H, $J = 5.34$ Hz, CH_3). ^{13}C NMR (75.45 MHz, $CDCl_3$, δ): 165.1, 154.7, 149.3, 148.1, 144.3, 142.8, 141.6, 138.1, 130.3, 130.2, 129.7, 129.4, 125.7, 125.0, 62.0, 14.3. Anal. Calc. for $C_{16}H_{13}N_3O_2$: N, 15.05; C, 68.81; H, 4.69. Found: N, 14.65; C, 68.36; H, 4.78%.

3.1.3. 1-(6-(Quinoxalin-2-yl)pyridine-2-yl)ethanone

Sodium (0.54 g, 23.2 mmol) was dissolved in 20 mL of freshly dried ethanol, then the excess ethanol was fully removed via vacuum. A solution of ethyl 6-(quinoxalin-2-yl)pyridine-2-carboxylate (1.30 g, 4.64 mmol) in freshly distilled ethyl acetate (30 mL) was added dropwise to the dry EtONa. The yellow mixture was refluxed for 8 h to become a brown solution. Concentrated HCl (20 mL) acid was added dropwise to the solution and resultant mixture was further refluxed for 10 h. After cooling to room temperature, 50 mL water was added and the aqueous phase was extracted with CH_2Cl_2 (5×20 mL). The mixture of combined organic phases was washed with a solution (30 mL) of 5% aqueous Na_2CO_3, and dried over anhydrous Na_2SO_4. The solvents were evaporated under reduced pressure, the residue was subsequently purified by column chromatography [silica gel; eluting reagent: light petroleum–EtOAc (8:1)]. The 1-(6-(quinoxalin-2-yl)pyridine-2-yl)ethanone was obtained as white solid (0.74 g) in 65% isolated yield. Mp: 115–116 °C. IR (KBr, cm^{-1}): 1694 (s, $\nu_{C=O}$), 1582, 1411, 1354, 1262, 1105, 764, 411. ^1H NMR (300 MHz, $CDCl_3$, δ): 10.10 (s, 1H, *o*-quinoxalin-H), 8.84 (d, 1H, $J = 7.77$ Hz, *Py*–H), 8.21 (d, 1H, $J = 7.86$ Hz, *Py*–H), 8.18 (m, 2H, quinoxalin-H), 8.08 (t, 1H, $J = 7.65$ Hz, *Py*–H), 7.85 (m, 2H, quinoxalin-H), 2.92 (s, 3H, $CH_3C{=}O$). ^{13}C NMR (75.45 MHz, $CDCl_3$, δ): 199.8, 153.8, 153.1, 149.3, 143.9, 142.7, 141.7, 138.1, 130.4, 130.3, 129.7, 129.4, 125.2, 122.3, 25.8. Anal. Calc. for $C_{15}H_{11}N_3O$: N, 16.86; C, 72.28; H, 4.45. Found: N, 16.80; C, 72.21; H, 4.45%.

3.2. Synthesis of 2-quinoxalinyl-6-iminopyridines

3.2.1. (E)-2,6-Dimethyl-N-(1-(6-(quinoxalin-2-yl)pyridin-2-yl)ethylidene)benzenamine (**L1**)

2,6-Dimethylaniline (0.39 mL, 3 mmol) was added to a solution of 1-(6-(quinoxalin-3-yl)pyridine-2-yl)ethanone (0.75 g, 3 mmol) with a catalytic amount of *p*-toluenesulfonic acid in toluene (50 mL). The mixture was refluxed for 12 h under nitrogen atmosphere. During this reaction, the water formed was eliminated by using a dean-Stark apparatus. After the solvent was evaporated under reduced pressure, the residue was separated by column chromatography with silica gel with an eluting reagent of light petroleum/EtOAc (8/1). The expected compound **L1** was obtained as yellow solid in 63% isolated yield (0.66 g). Mp: 142–143 °C. IR (KBr, cm^{-1}): 1642 (s, $\nu_{C=N}$), 1568, 1552, 1464, 1360, 1203, 765, 405. ^1H NMR (300 MHz, $CDCl_3$, δ): 10.11 (s, 1H, *o*-quinoxalin-H), 8.74 (d, 1H, $J = 7.45$ Hz, *Py*–H), 8.53 (d, 1H, $J = 7.83$ Hz, *Py*–H), 8.19 (m, 2H, quinoxalin-H), 8.04 (t, 1H, $J = 7.92$ Hz, *Py*–H), 7.82 (m, 2H, quinoxalin-H), 7.11 (d, 2H, $J = 7.47$ Hz, *Ph*–H), 6.98 (t, 1H, $J = 7.17$ Hz, *Ph*–H), 2.38 (s, 3H, $N{=}C{-}CH_3$), 2.09 (s, 6H, $-CH_3$). ^{13}C NMR (75.45 MHz, $CDCl_3$, δ): 168.6, 157.4, 154.8, 151.5, 150.2, 145.7, 144.2, 143.3, 139.2, 131.7, 131.6, 131.2, 130.9, 129.4, 126.9, 124.6, 124.5, 123.6, 19.5, 18.1. Anal. Calc. for $C_{23}H_{20}N_4$: N, 15.90; C, 78.38; H, 5.72. Found: N, 15.60; C, 78.16; H, 5.75%.

3.2.2. (E)-2,6-Diethyl-N-(1-(6-(quinoxalin-2-yl)pyridin-2-yl)ethylidene)benzenamine (**L2**)

Using the same procedure as for the synthesis of **L1**, **L2** was obtained as yellow powder in 39% yield. Mp: 155–156 °C. IR (KBr, cm^{-1}): 1645 (s, $\nu_{C=N}$), 1567, 1546, 1451, 1363, 1244, 1197, 1111, 1060, 828, 757, 406. ^1H NMR (300 MHz, $CDCl_3$, δ): 10.13 (s, 1H, *o*-quinoxalin-H), 8.77 (d, 1H, $J = 7.65$ Hz, *Py*–H), 8.55 (d, 1H, $J = 7.83$ Hz, *Py*–H), 8.22 (m, 2H, quinoxalin-H), 8.07 (t, 1H, $J = 7.80$ Hz, *Py*–H), 7.86 (m, 2H, quinoxalin-H), 7.18 (d, 2H, $J = 7.86$ Hz, *Ph*–H), 7.09 (t, 1H, $J = 6.54$ Hz, *Ph*–H), 2.48 (m, 4H, –CH_2–), 2.39 (s, 3H, $N{=}C{-}CH_3$), 1.20 (t, 6H, $J = 7.47$ Hz, CH_3). ^{13}C NMR

(75.45 MHz, $CDCl_3$, δ): 166.8, 155.9, 153.4, 150.0, 147.7, 144.3, 142.7, 141.8, 137.7, 131.2, 130.2, 130.1, 129.7, 129.4, 129.0, 128.2, 126.0, 125.3, 123.4, 122.9, 122.1, 24.6, 21.5, 16.9, 13.7. Anal. Calc. for $C_{25}H_{24}N_4$: N, 14.73; C, 78.92; H, 6.36. Found: N, 14.50; C, 79.30; H, 6.49%.

3.2.3. (E)-2,6-Diisopropyl-N-(1-(6-(quinoxalin-2-yl)-pyridin-2-yl)ethylidene)benzenamine (L3)

Using the same procedure as for the synthesis of **L1**, **L3** was obtained as yellow powder in 74% yield. Mp: 215–216 °C. IR (KBr, cm^{-1}): 1637 (s, $\nu_{C=N}$), 1568, 1458, 1361, 1241, 1112, 1059, 829, 758, 406. ^1H NMR (300 MHz, $CDCl_3$, δ):10.11 (s, 1H, *o*-quinoxalin-H), 8.74 (d, 1H, $J = 7.68$ Hz, *Py*–H), 8.51 (d, 1H, $J = 7.89$ Hz, *Py*–H), 8.20 (m, 2H, quinoxalin-H), 8.04 (t, 1H, $J = 7.80$ Hz, *Py*–H), 7.82 (m, 2H, quinoxalin-H), 7.17 (m, 3H, *Ph*–H), 2.80 (m, 2H, $CH(CH_3)_2$), 2.38 (s, 3H, N=C–CH_3), 1.20 (s, 12H, CH_3). ^{13}C NMR (75.45 MHz, $CDCl_3$, δ): 166.8, 155.9, 153.4, 150.0, 146.4, 144.3, 142.7, 141.8, 137.7, 135.8, 130.2, 130.1, 129.7, 129.4, 123.7, 123.0, 122.9, 122.1, 28.3, 23.2, 22.9, 17.3. Anal. Calc. for $C_{27}H_{28}N_4$: N, 13.71; C, 79.38; H, 6.91. Found: N, 13.69; C, 78.99; H, 6.84%.

3.2.4. (E)-2,4,6-Trimethyl-N-(1-(6-(quinoxalin-2-yl)-pyridin-2-yl)ethylidene)benzenamine (L4)

Using the same procedure as for the synthesis of **L1**, **L4** was obtained as yellow powder in 28% yield. Mp: 132–133 °C. IR (KBr, cm^{-1}): 1645 (s, $\nu_{C=N}$), 1568, 1546, 1476, 1361, 1217, 1112, 824, 763, 409. ^1H NMR (300 MHz, $CDCl_3$, δ): 10.12 (s, 1H, *o*-quinoxalin-H), 8.74 (d, 1H, $J = 7.89$ Hz, *Py*–H), 8.52 (d, 1H, $J = 7.92$ Hz, *Py*–H), 8.21 (m, 2H, quinoxalin-H), 8.04 (t, 1H, $J = 7.95$ Hz, *Py*–H), 7.84 (m, 2H, quinoxalin-H), 6.94 (s, 2H, *Ph*–H), 2.36 (s, 3H, N=C–CH_3), 2.33 (s, 3H, *p*-CH_3), 2.06 (s, 6H, *o*-CH_3). ^{13}C NMR (75.45 MHz, $CDCl_3$, δ): 166.9, 155.7, 152.9, 149.7, 145.8, 143.9, 142.3, 141.5, 137.3, 131.9, 129.8, 129.7, 129.4, 129.0, 128.2, 124.9, 122.6, 121.7, 20.4, 17.5, 16.2. Anal. Calc. for $C_{24}H_{22}N_4$: N, 15.29; C, 78.66; H, 6.05. Found: N, 14.99; C, 78.38; H, 6.11%.

3.2.5. (E)-2,6-Difluoro-N-(1-(6-(quinoxalin-2-yl)pyridin-2-yl)ethylidene)benzenamine (L5)

Using the same procedure as for the synthesis of **L1**, **L5** was obtained as yellow powder in 40% yield. Mp: 163–164 °C. IR (KBr, cm^{-1}): 1639 (s, $\nu_{C=N}$), 1567, 1469, 1365, 998, 829, 766, 741, 406. ^1H NMR (300 MHz, $CDCl_3$, δ): 10.09 (s, 1H, *o*-quinoxalin-H), 8.74 (d, 1H, $J = 7.8$ Hz, *Py*–H), 8.49 (d, 1H, $J = 7.83$ Hz, *Py*–H), 8.19 (m, 2H, quinoxalin-H), 8.03 (t, 1H, J = 7.83 Hz, *Py*–H), 7.82 (m, 2H, quinoxalin-H), 7.01 (m, 3H, *Ph*–H), 2.57 (s, 3H, N=C–CH_3). ^{13}C NMR (75.45 MHz, $CDCl_3$, δ): 172.5, 155.3, 154.2, 153.4, 151.8, 149.8, 144.2, 142.6, 141.8, 137.7, 130.2, 130.2, 129.7, 129.4, 124.2, 123.4, 122.8, 111.8, 111.5, 17.7. Anal. Calc. for $C_{21}H_{14}F_2N_4$: N, 15.55; C, 69.99; H, 3.92. Found: N, 15.48; C, 69.52; H, 3.92%.

3.2.6. (E)-2,6-Dichloro-N-(1-(6-(quinoxalin-2-yl)pyridin-2-yl)ethylidene)benzenamine (L6)

In the condensation reaction of 2.4 mmol 2,6-dichloroaniline (0.39 g) with 2 mmol 1-(6-(quinoxalin-2-yl)pyridine-2-yl)ethanone (0.50 g) in 30 mL of toluene along with 3 mL of tetraethyl silicate as the water absorbent, compound **L6** was obtained as yellow powder in 31% yield (0.24 g). Mp: 194–195 °C. IR (KBr, cm^{-1}): 1651 (s, $\nu_{C=N}$), 1565, 1555, 1433, 1362, 1224, 1115, 1063, 819, 765, 408. ^1H NMR (300 MHz, $CDCl_3$, δ): 10.13 (s, 1H, *o*-quinoxalin-H), 8.80 (d, 1H, $J = 7.74$ Hz, *Py*–H), 8.57 (d, 1H, $J = 7.68$ Hz, *Py*–H), 8.21 (m, 2H, quinoxalin-H), 8.15 (m, 1H, *Py*–H), 7.85 (m, 2H, quinoxalin-H), 7.33 (d, 2H, $J = 8.01$ Hz, *Ph*–H), 7.02 (t, 1H, $J = 7.74$ Hz, *Ph*–H), 2.51 (s, 3H, N=C–CH_3). ^{13}C NMR (75.45 MHz, $CDCl_3$, δ): 171.2, 155.0, 153.4, 149.7, 145.6, 144.1, 142.6, 141.8, 137.8, 130.2, 130.1, 129.7, 129.3, 128.2, 124.5, 124.4, 123.5, 122.8, 17.7. Anal. Calc. for $C_{21}H_{14}Cl_2N_4$: N, 14.25; C, 64.14; H, 3.59. Found: N, 13.81; C, 64.04; H, 3.65%.

3.2.7. (E)-2,6-Dibromo-N-(1-(6-(quinoxalin-2-yl)pyridin-2-yl)ethylidene)benzenamine (L7)

Using the same procedure as for the synthesis of **L6**, **L7** was obtained as yellow powder in 26% yield. Mp: 206–207 °C. IR (KBr, cm^{-1}): 1650 (s, $\nu_{C=N}$), 1565, 1547, 1426, 1363, 1224, 1114, 1063, 821, 763, 727, 408. ^1H NMR (300 MHz, $CDCl_3$, δ): 10.10 (s, 1H, *o*-quinoxalin-H), 8.77 (d, 1H, $J = 7.84$ Hz, *Py*–H), 8.54 (d, 1H, $J = 7.8$ Hz, *Py*–H), 8.19 (m, 2H, quinoxalin-H), 8.05 (t, 1H, *Py*–H), 7.82 (m, 2H, quinoxalin-H), 7.60 (d, 2H, $J = 8.04$ Hz, *Ph*–H), 6.88 (t, 1H, $J = 7.96$ Hz, *Ph*–H), 2.46 (s, 3H, N=C–CH_3). ^{13}C NMR (75.45 MHz, $CDCl_3$, δ): 170.9, 155.1, 153.6, 149.9, 148.1, 144.2, 142.7, 141.9, 137.9, 132.0, 130.2, 130.1, 129.8, 129.4, 125.3, 123.6, 122.9, 113.6, 17.7. Anal. Calc. for $C_{21}H_{14}Br_2N_4$: N, 11.62; C, 52.31; H, 2.93. Found: N, 11.64; C, 52.46; H, 2.95%.

3.3. Synthesis of metal complexes

3.3.1. Synthesis of (L)$FeCl_2$ (1–7)

Iron complexes **1**–**7** were synthesized by the reaction of $FeCl_2 \cdot 4H_2O$ with the corresponding ligands in THF. A typical synthetic procedure for complex **1** is described as follows. A mixture of $FeCl_2 \cdot 4H_2O$ (0.040 g, 0.20 mmol) with compound **L1** (0.071 g, 0.20 mmol) in freshly distilled THF (5 mL) was stirred at room temperature for 12 h under nitrogen atmosphere. The precipitate was formed, collected through a filter, and washed with freshly distilled diethyl ether. After drying in vacuum, iron(II) complex **1** was obtained as the blue powder in 95% yield (0.092 g). IR (KBr, cm^{-1}): 1623 (m, $\nu_{C=N}$), 1592, 1371, 1213, 778, 763, 411. Anal. Calc. for $C_{23}H_{20}Cl_2FeN_4 \cdot 3H_2O$: N, 10.51; C, 51.81; H, 4.91. Found: N, 11.11; C, 51.41; H, 5.08%. $\mu_{eff} = 6.2$ μ_B. Data for complex **2** are as follows. Yield: 42%. IR (KBr, cm^{-1}): 1609 (w, $\nu_{C=N}$), 1589, 1501, 1482, 1374, 1273, 1198, 1129, 1094, 910, 817, 770, 413.

Anal. Calc. for $C_{25}H_{24}Cl_2FeN_4$: N, 11.05; C, 59.20; H, 4.77. Found: N, 10.73; C, 58.74; H, 4.78%. Data for complex **3** are as follows. Yield: 65%. IR (KBr, cm^{-1}): 1613 (w, $\nu_{C=N}$), 1589, 1498, 1444, 1371, 1273, 1196, 1092, 820, 798, 774, 411. Anal. Calc. for $C_{27}H_{28}Cl_2FeN_4$: N, 10.47; C, 60.58; H, 5.27. Found: N, 10.01; C, 59.93; H, 5.24%. $\mu_{eff} = 6.6$ μ_B. Data for complex **4** are as follows. Yield: 96%. IR (KBr, cm^{-1}): 1609 (w, $\nu_{C=N}$), 1591, 1503, 1371, 1274, 1218, 1093, 825, 762, 440. Anal. Calc. for $C_{24}H_{22}Cl_2FeN_4$: N, 11.36; C, 58.45; H, 4.50. Found: N, 11.30; C, 58.63; H, 5.04%. $\mu_{eff} = 5.6$ μ_B. Data for complex **5** are as follows. Yield: 56%. IR (KBr, cm^{-1}): 1614 (w, $\nu_{C=N}$), 1591, 1498, 1471, 1371, 1279, 1225, 1143, 1094, 1006, 816, 773, 413. Anal. Calc. for $C_{21}H_{14}Cl_2F_2FeN_4$: N, 11.50; C, 51.78; H, 2.90. Found: N, 11.19; C, 51.41; H, 2.94%. $\mu_{eff} = 5.7$ μ_B. Data for complex **6** are as follows. Yield: 71%. IR (KBr, cm^{-1}): 1629 (w, $\nu_{C=N}$), 1592, 1501, 1435, 1370, 1275, 1228, 1142, 1093, 819, 792, 769, 740, 415. Anal. Calc. for $C_{21}H_{14}Cl_4FeN_4$: N, 10.77; C, 48.50; H, 2.71. Found: N, 11.00; C, 48.15; H, 2.71%. $\mu_{eff} = 6.6$ μ_B. Data for complex **7** are as follows. Yield: 74%. IR (KBr, cm^{-1}): 1624 (w, $\nu_{C=N}$), 1590, 1550, 1502, 1427, 1370, 1276, 1223, 1140, 1096, 818, 791, 768, 729, 416. Anal. Calc. for $C_{21}H_{14}Br_2Cl_2FeN_4$: N, 9.20; C, 41.42; H, 2.32. Found: N, 9.21; C, 40.99; H, 2.53%. $\mu_{eff} = 5.8$ μ_B.

3.3.2. Synthesis of (*L*) $CoCl_2$ (*8–14*)

Cobalt complexes **8–14** were prepared by the same synthetic procedures for iron complexes **1–7** and obtained as green powder. The synthetic procedure of **8** can be described as follows: to a mixture of ligand **L1** (0.071 g, 0.20 mmol) and $CoCl_2$ (0.026 g, 0.20 mmol) was added freshly distilled THF (5 mL) at room temperature. The solution turned green immediately. The reaction mixture was stirred for 6 h, and the precipitate was collected by filtration and washed with diethyl ether, followed by drying in vacuum. The desired complex was obtained as green powder in 78% yield. IR (KBr, cm^{-1}): 1624 (w, $\nu_{C=N}$), 1592, 1502, 1481, 1372, 1273, 1213, 1093, 819, 774, 414. Anal. Calc. For $C_{23}H_{20}Cl_2CoN_4$: N, 11.62; C, 57.28; H, 4.18. Found: N, 11.79; C, 56.95; H, 4.32%. $\mu_{eff} = 6.4$ μ_B. Data for complex **9** are as follows. Yield: 73%. IR (KBr, cm^{-1}): 1611 (w, $\nu_{C=N}$), 1589, 1480, 1442, 1371, 1270, 1213, 1198, 1092, 816, 771, 415. Anal. Calc. for: $C_{25}H_{24}Cl_2CoN_4$: N, 10.98; C, 58.84; H, 4.74. Found: N, 10.75; C, 58.51; 4.70%. Data for complex **10** are as follows. Yield: 74%. IR (KBr, cm^{-1}): 1618 (w, $\nu_{C=N}$), 1592, 1370, 1272, 1212, 1200, 1091, 817, 769, 415. Anal. Calc. for $C_{27}H_{28}Cl_2CoN_4$: N, 10.41; C, 60.23; H, 5.24. Found: N, 10.32; C, 60.38; H, 5.05%. $\mu_{eff} = 5.8$ μ_B. Data for complex **11** are as follows. Yield: 72%. IR (KBr, cm^{-1}): 1616 (w, $\nu_{C=N}$), 1591, 1482, 1368, 1219, 1092, 1022, 826, 763, 742, 411. Anal. Calc. for $C_{24}H_{22}Cl_2CoN_4$: N, 11.29; C, 58.08; H, 4.47. Found: N, 11.27; C, 58.52; H, 4.21%. $\mu_{eff} = 5.7$ μ_B. Data for complex **12** are as follows. Yield: 72%. IR (KBr, cm^{-1}): 1634 (w, $\nu_{C=N}$), 1591, 1471, 1371, 1278, 1225, 1094, 1006, 781, 415. Anal. Calc. for $C_{21}H_{14}F_2Cl_2CoN_4$: N, 11.43; C, 51.45; H, 2.88. Found: N, 11.23; C, 51.68; H, 2.86%. $\mu_{eff} = 6.3$ μ_B. Data for complex **13** are as follows. Yield: 75%. IR (KBr, cm^{-1}): 1631 (w, $\nu_{C=N}$), 1592, 1436, 1369, 1272, 1229, 1092, 819, 792, 769, 731, 416. Anal. Calc. for $C_{21}H_{14}Cl_4CoN_4$: N, 10.71; C, 48.22; H, 2.70. Found: N, 10.50; C, 47.76; H, 2.77%. $\mu_{eff} = 6.2$ μ_B. Data for complex 14 are as follows. Yield: 69%. IR (KBr, cm^{-1}): 1627 (w, $\nu_{C=N}$), 1591, 1501, 1481, 1426, 1370, 1273, 1224, 1141, 1094, 819, 768, 728, 418. Anal. Calc. for $C_{21}H_{14}Br_2Cl_2CoN_4$: N, 9.15; C, 41.21; H, 2.31. Found: N, 8.96; C, 40.83; H, 2.41%. $\mu_{eff} = 5.6$ μ_B.

3.4. X-ray crystallographic studies

The crystals of compound **L1** and **L4** suitable for single-crystal X-ray diffraction analysis were grown by slow evaporation of its hexane–EtOAc (8:1) solution in NMR tube, while crystals of complexes **1**, **4**, **10** and **13** suitable for X-ray diffraction analysis were obtained by slow diffusion of Et_2O into their methanol solutions at room temperature under nitrogen atmosphere. With graphite-monochromated Mo Kα radiation ($\lambda = 0.71073$ Å) at 293(2) K, the intensity data for crystals of **L1**, **L4** and **10** were carried out on a Bruker SMART 1000 CCD diffractometer, and the data for crystals of **1** and **13** were collected on a Rigaku RAXIS Rapid IP diffractometer while the data for crystal of **4** was collected on Siemens Smart. Cell parameters were obtained by global refinement of the positions of all collected reflections. Intensities were corrected for Lorentz and polarization effects and empirical absorption. The structures were solved by direct methods and refined by full-matrix least squares on F^2. All non-hydrogen atoms were refined anisotropically. All hydrogen atoms were placed in calculated positions. Structure solution and refinement were performed by using the SHELXL-97 package [27]. The crystal data collection and refinement data for ligand **L1**, **L4** and complexes **1**, **4**, **10**, **13** are summarized in Table 8.

3.5. Procedure for ethylene oligomerization

3.5.1. Ethylene oligomerization at ambient pressure

The pre-catalyst (5 μmol) was added to a Schlenk-type flask under nitrogen atmosphere. After the flask was evacuated-filled three times with nitrogen and final one with ethylene, then charged with 30 mL of fleshly distilled toluene. The mixture was intensively stirred for 5 min at setting temperature. The required amount of activator was subsequently added, and the reaction solution was intensively stirred for desired period of time under 1 atm of ethylene during the entire experiment. The reaction was terminated with 50 mL acidified ethanol. The organic layer was analyzed by using gas chromatography.

3.5.2. Ethylene oligomerization at elevated pressure

The ethylene oligomerization at elevated-pressure was performed in a stainless autoclave (500 mL) through

Table 8
Crystal data and structure refinement for compound **L1**, **L4**, **1**, **4**, **10**, **13**

Data	**L1**	**L4**	**1** · Et_2O	**4** · $0.5Et_2O$	**10**	**13**
Formula	$C_{23}H_{20}N_4$	$C_{24}H_{21}N_4$	$C_{27}H_{30}Cl_2FeN_4O$	$C_{26}H_{27}Cl_2FeN_4O_{0.5}$	$C_{27}H_{28}CoCl_2N_4$	$C_{21}H_{14}Cl_4CoN_4$
Formula weight	352.43	365.45	553.30	530.27	538.36	523.09
Color	Yellow	Yellow	Black	Black	Black	Black
Temperature (K)	294(2)	293(2)	293(2)	293(2)	293(2)	293(2)
Crystal system	Triclinic	Triclinic	Monoclinic	Monoclinic	Monoclinic	Orthorhombic
Space group	$P\bar{1}$	$P\bar{1}$	$P21/c$	$C2/c$	$P2(1)/c$	$Fdd2$
a (Å)	7.621(2)	8.1766(2)	9.3848(2)	26.068(5)	9.6406(1)	31.2837(7)
b (Å)	11.455(3)	9.3682(2)	16.517(3)	11.744(2)	15.413(2)	31.9642(7)
c (Å)	11.567(3)	13.7087(3)	16.998(3)	18.709(3)	17.516(3)	8.7312(2)
α (°)	99.315(5)	86.4580(1)	90	90	90	90
β (°)	96.938(5)	78.1780(1)	104.75(3)	119.291(2)	93.868(3)	90
γ (°)	99.134(5)	82.0770(1)	90	90	90	90
V (Å^3)	972.6(5)	1017.39(4)	2548.0(8)	4995.4(2)	2596.7(7)	8730.8(3)
Z	2	2	4	8	4	16
Wavelength (Å)	0.71073	0.71073	0.71073	0.71073	0.71073	0.71073
D_{calc} (mg m^{-3})	1.203	1.193	1.442	1.410	1.377	1.592
Crystal size (mm)	$0.60 \times 0.50 \times 0.40$	$0.56 \times 0.43 \times 0.19$	$0.25 \times 0.21 \times 0.07$	$0.51 \times 0.23 \times 0.10$	$0.20 \times 0.08 \times 0.08$	$0.30 \times 0.30 \times 0.10$
θ Range (°)	1.80–26.44	2.20–28.32	2.24–27.48	1.79–25.01	1.76–26.33	1.82–28.30
Limiting indices	$-7 \leqslant h \leqslant 9$, $-12 \leqslant k \leqslant 14$, $-14 \leqslant l \leqslant 10$	$-10 \leqslant h \leqslant 9$, $-12 \leqslant k \leqslant 12$, $-12 \leqslant l \leqslant 18$	$0 \leqslant h \leqslant 12$, $0 \leqslant k \leqslant 21$, $-22 \leqslant l \leqslant 21$	$-30 \leqslant h \leqslant 30$, $-10 \leqslant k \leqslant 13$, $-15 \leqslant l \leqslant 22$	$-11 \leqslant h \leqslant 12$, $-19 \leqslant k \leqslant 18$, $-17 \leqslant l \leqslant 21$	$-41 \leqslant h \leqslant 37$, $-40 \leqslant k \leqslant 41$, $-11 \leqslant l \leqslant 11$
Reflections collected/unique	5438/3898	9953/4976	22,435/6042	11,912/4393	14,375/5255	11,687/4526
R_{int}	0.0246	0.0232	0.0640	0.0578	0.0598	0.0290
Data/restraints/parameters	3898/0/244	4976/0/253	5822/7/316	4393/0/303	5255/0/307	4526/1/271
Absorption coefficient (mm^{-1})	0.073	0.072	0.830	0.842	0.889	1.292
F_{000}	372	386	1152	2200	1116	4208
Final R indices [$(I) > 2\sigma(I)$]	$R_1 = 0.0525$, $wR_2 = 0.1325$	$R_1 = 0.0493$, $wR_2 = 0.1638$	$R_1 = 0.0665$, $wR_2 = 0.1554$	$R_1 = 0.0833$, $wR_2 = 0.1765$	$R_1 = 0.0445$, $wR_2 = 0.0882$	$R_1 = 0.0304$, $wR_2 = 0.0641$
R indices (all data)	$R_1 = 0.1106$, $wR_2 = 0.1669$	$R_1 = 0.0754$, $wR_2 = 0.1807$	$R_1 = 0.1348$, $wR_2 = 0.1802$	$R_1 = 0.1065$, $wR_2 = 0.1896$	$R_1 = 0.1155$, $wR_2 = 0.1117$	$R_1 = 0.0439$, $wR_2 = 0.0667$
Goodness-of-fit	1.011	1.131	0.952	1.030	0.993	0.985
Largest difference in peak and hole (e Å^{-3})	0.227 and −0.194	0.227 and −0.190	0.680 and −0.360	0.625 and −0.603	0.379 and −0.284	0.329 and −0.248

a solenoid clave by continuous feeding of ethylene at desired pressures. The complex (5 μmol) was dissolved in 100 mL of freshly distilled toluene under nitrogen atmosphere, and the solution was subsequently transferred to the fully dried reactor via a syringe. The required amount of activator was then injected into the reactor, and the reaction mixture was intensively stirred for the desired time under corresponding pressure of ethylene during the entire experiment. The reaction was terminated and analyzed by using the same method as described above for the reaction with 1 atm ethylene.

Acknowledgements

This work was supported by NSFC No. 20674089 and MOST 2006AA03Z553. M.A. is grateful to the Chinese Academy of Science (CAS) and The Academy of Science for The Developing World (TWAS) for the Postgraduate Fellowships.

Appendix A. Supplementary material

CCDC 639003, 639004, 639005, 639006, 639007 and 639008 contain the supplementary crystallographic data for **L1**, **L4**, **1**, **4**, **10** and **13**. These data can be obtained free of charge via http://www.ccdc.cam.ac.uk/conts/retrieving.html, or from the Cambridge Crystallographic Data Centre, 12 Union Road, Cambridge CB2 1EZ, UK; fax: (+44) 1223-336-033; or e-mail: deposit@ccdc.cam.ac.uk. Supplementary data associated with this article can be found, in the online version, at doi:10.1016/j.jorganchem.2007.04.027.

References

[1] (a) D. Vogt, in: B. Cornils, W.A. Herrmann (Eds.), Applied Homogeneous Catalysis with Organometallic Compounds, vol. 1, VCH, Weinheim, 2002, p. 240;
(b) W. Keim, F.H. Kowaldt, R. Goddard, C. Krüger, Angew. Chem. 90 (1978) 493;

Angew. Chem., Int. Ed. Engl. 17 (1978) 466;
(c) W. Keim, A. Behr, B. Limbacker, C. Krüger, Angew. Chem., Int. Ed. Engl. 22 (1983) 503.
[2] (a) W.K. Reagen, Am. Chem. Soc. Symp., Div. Petrol. Chem. 34 (1989) 583, 3;
(b) W.K. Reagen, B.K. Conroy, Phillips Petroleum, US 5.288.823, 1994;
(c) Eur. Chem. News 2000, 2–8 October, 29.
[3] (a) A. Bollmann, K. Blann, J.T. Dixon, F.M. Hess, E. Killian, H. Maumela, D.S. McGuinness, D.H. Morgan, A. Neveling, S. Otto, M. Overett, A.M.Z. Slawin, P. Wasserscheid, S. Kuhlmann, J. Am. Chem. Soc. 126 (2004) 14712;
(b) M.J. Overett, K. Blann, A. Bollmann, J.T. Dixon, D. Haasbroek, E. Killian, H. Maumela, D.S. McGuinness, D.H. Morgan, J. Am. Chem. Soc. 127 (2005) 10723.
[4] (a) W. Keim, A. Behr, G. Kraus, J. Organomet. Chem. 251 (1983) 377;
(b) W. Keim, Angew. Chem., Int. Ed. Engl. 29 (1990) 235;
(c) M. Peuckert, W. Keim, Organometallics 2 (1983) 594;
(d) W. Keim, R.P. Schulz, J. Mol. Catal. A: Chem. 92 (1994) 21.
[5] (a) S.D. Ittel, L.K. Johnson, M. Brookhart, Chem. Rev. 100 (2000) 1169;
(b) S. Mecking, Angew. Chem. Int. Ed. 40 (2001) 534;
(c) V.C. Gibson, S.K. Spitzmesser, Chem. Rev. 103 (2003) 283;
(d) F. Speiser, P. Braustein, L. Saussine, Acc. Chem. Res. 38 (2005) 784;
(e) W. Zhang, W. Zhang, W.-H. Sun, Prog. Chem. 17 (2005) 310;
(f) S. Jie, S. Zhang, W.-H. Sun, Petrochem. Tech. (Shiyou Huagong) 35 (2006) 295;
(g) W.-H. Sun, D. Zhang, S. Zhang, S. Jie, J. Hou, Kinet. Catal. 47 (2006) 278.
[6] (a) G.J.P. Britovsek, V.C. Gibson, B.S. Kimberley, P.J. Maddox, S.J. McTavish, G.A. Solan, A.J.P. White, D.J. Williams, Chem. Commun. (1998) 849;
(b) B.L. Small, M. Brookhart, A.M.A. Bennett, J. Am. Chem. Soc. 120 (1998) 4049.
[7] (a) G.J.P. Britovsek, V.C. Gibson, B.S. Kimberley, S. Mastroianni, C. Redshaw, G.A. Solan, A.J.P. White, D.J.J. Williams, Chem. Soc., Dalton Trans. (2001) 1639;
(b) G.J.P. Britovsek, S. Mastroianni, G.A. Solan, S.P.D. Baugh, C. Redshaw, V.C. Gibson, A.J.P. White, D.J. Williams, M.R.J. Elsegood, Chem. Eur. J. 6 (2000) 2221;
(c) R. Souane, F. Isel, F. Peruch, P.J. Lutz, C.R. Chim. 5 (2002) 43;
(d) Z. Ma, W.-H. Sun, Z. Li, C. Shao, Y. Hu, X. Li, Polym. Int. 51 (2002) 994;
(e) A.S. Ionkin, W.J. Marshall, D.J. Adelman, B.B. Fones, B.M. Fish, M.F. Schiffhauer, Organometallics 25 (2006) 2978;
(f) C. Bianchini, G. Mantovani, A. Meli, F. Migliacci, F. Laschi, Organometallics 22 (2003) 2545;
(g) B.L. Small, Organometallics 22 (2003) 3178;
(h) M.E. Bluhm, C. Folli, M. Döring, J. Mol. Catal. A: Chem. 212 (2004) 13;
(i) I. Kim, B.H. Han, Y.S. Ha, C.S. Ha, D.W. Park, Catal. Today 93 (2004) 281;
(j) C. Bianchini, G. Giambastiani, I.R. Guerrero, A. Meli, E. Passaglia, T. Gragnoli, Organometallics 23 (2004) 6087;
(k) M.J. Overett, R. Meijboom, J.R. Moss, Dalton Trans. (2005) 551.
[8] (a) N. Kleigrewe, W. Steffen, T. Blömker, G. Kehr, R. Fröhlich, B. Wibbeling, G. Erker, J.-C. Wasilke, G. Wu, G.C. Bazan, J. Am. Chem. Soc. 127 (2005) 13955;
(b) M.W. Bouwkamp, E. Lobkovsky, P.J. Chirik, J. Am. Chem. Soc. 127 (2005) 9660;
(c) J. Scott, S. Gambarotta, I. Korobkov, P.H.M. Budzelaar, Organometallics 24 (2005) 6298;
(d) G.J.P. Britovsek, M. Bruce, V.C. Gibson, B.S. Kimberley, P.J. Maddox, S. Mastroianni, S.J. McTavish, C. Redshaw, G.A. Solan, S. Strömberg, A.J.P. White, D.J. Williams, J. Am. Chem. Soc. 121 (1999) 8728;
(e) B.L. Small, M. Brookhart, Macromolecules 32 (1999) 2120;
(f) L. Deng, P. Margl, T. Ziegler, J. Am. Chem. Soc. 121 (1999) 6479;
(g) D.V. Khoroshun, D.G. Musaev, T. Vreven, K. Morokuma, Organometallics 20 (2001) 2007;
(h) T.Z. Zhang, W.-H. Sun, T. Li, X.Z. Yang, J. Mol. Catal. A: Chem. 218 (2004) 119.
[9] G.J.P. Britovsek, V.C. Gibson, D.F. Wass, Angew. Chem., Int. Ed. 38 (1999) 428.
[10] (a) G.J.P. Britovsek, V.C. Gibson, O.D. Hoarau, S.K. Spitzmesser, A.J.P. White, D.J. Williams, Inorg. Chem. 42 (2003) 3454;
(b) R. Cowdell, C.J. Davies, S.J. Hilton, J.-D. Maréchal, G.A. Solan, O. Thomas, J. Fawcett, Dalton Trans. (2004) 3231;
(c) L. LePichon, D.W. Stephan, X. Gao, Q. Wang, Organometallics 21 (2002) 1362;
(d) W.-H. Sun, X. Tang, T. Gao, B. Wu, W. Zhang, H. Ma, Organometallics 23 (2004) 5037;
(e) M.-S. Zhou, S.-P. Huang, L.-H. Weng, W.-H. Sun, D.-S. Liu, J. Organomet. Chem. 665 (2003) 237.
[11] (a) L. Wang, W.-H. Sun, L. Han, H. Yang, Y. Hu, X. Jin, J. Organomet. Chem. 658 (2002) 62;
(b) G.J.P. Britovsek, S.P.D. Baugh, O. Hoarau, V.C. Gibson, D.F. Wass, A.J.P. White, D.J. Williams, Inorg. Chim. Acta 345 (2003) 279.
[12] W.-H. Sun, S. Jie, S. Zhang, W. Zhang, Y. Song, H. Ma, J. Chen, K. Wedeking, R. Fröhlich, Organometallics 25 (2006) 666.
[13] J.D.A. Pelletier, Y.D.M. Champouret, J. Cadarso, L. Clowes, M. Gañete, K. Singh, V. Thanarajasingham, G.A. Solan, J. Organomet. Chem. 691 (2006) 4114.
[14] S. Jie, S. Zhang, K. Wedeking, W. Zhang, H. Ma, X. Lu, Y. Deng, W.-H. Sun, C.R. Chim. 9 (2006) 1500.
[15] W.-H. Sun, S. Zhang, S. Jie, W. Zhang, Y. Li, H. Ma, J. Chen, K. Wedeking, R. Fröhlich, J. Organomet. Chem. 691 (2006) 4196.
[16] (a) W.-H. Sun, P. Hao, S. Zhang, Q. Shi, W. Zuo, X. Tang, X. Lu, Organometallics 26 (2007) 2720;
(b) P. Hao, S. Zhang, W.-H. Sun, Q. Shi, S. Adewuyi, X. Lu, P. Li, Organometallics 26 (2007) 2439.
[17] W.-H. Sun, X. Tang, T. Gao, B. Wu, W. Zhang, H. Ma, Organometallics 23 (2004) 5037.
[18] S. Zhang, I. Vystorop, Z. Tang, W.-H. Sun, Organometallics 26 (2007) 2456.
[19] (a) Y. Cui, X. Tang, C. Shao, J. Li, W.-H. Sun, Chin. J. Chem. 23 (2005) 589;
(b) C. Shao, W.-H. Sun, Z. Li, Y. Hu, L. Han, Catal. Commun. 3 (2002) 405.
[20] X. Tang, W.-H. Sun, T. Gao, J. Hou, J. Chen, W. Chen, J. Organomet. Chem. 690 (2005) 1570.
[21] B.S. Furniss, A.J. Hannaford, P.W.G. Smith, A.R. Tatchell, Textbook of Practical Organic Chemistry, fifth ed., Person Education Limited, 1989, pp. 1189.
[22] X. Tang, Y. Cui, W.-H. Sun, Z. Miao, S. Yan, Polym. Int. 53 (2004) 2155.
[23] B.S. Furniss, A.J. Hannaford, P.W.G. Smith, A.R. Tatchell, Textbook of Practical Organic Chemistry, fifth ed., Person Education Limited, 1989, pp. 1052.
[24] (a) D.F. Evans, J. Chem. Soc. (1959) 2003;
(b) J. Löliger, R. Scheffold, J. Chem. Educ. 49 (1972) 646;
(c) S.K. Sur, J. Magn. Reson. 82 (1989) 169.
[25] Y. Chen, R. Chen, C. Qian, X. Dong, J. Sun, Organometallics 22 (2003) 4312.
[26] (a) E.Y.-X. Chen, T.J. Marks, Chem. Rev. 100 (2000) 1391;
(b) A.R. Karam, E.L. Catarí, F. López-Linares, G. Agrifoglio, C.L. Albano, A. Díaz-Barrios, T.E. Lehmann, S.V. Pekerar, L.A. Albornoz, R. Atencio, T. González, H.B. Ortega, P. Joskowics, Appl. Catal. A: Gen. 280 (2005) 165.
[27] G.M. Sheldrick, SHELXTL-97, Program for the Refinement of Crystal Structures, University of Gottingen, Germany, 1997.